

## In-beam gamma-ray spectroscopy of $^{74}\text{Se}$ following the $^{60}\text{Ni}(^{16}\text{O}, 2p)$ , $^{64}\text{Ni}(^{12}\text{C}, 2n)$ and $^{65}\text{Cu}(^{11}\text{B}, 2n)$ reactions

R. B. Piercey, A. V. Ramayya, R. M. Ronningen,\* J. H. Hamilton, and V. Maruhn-Rezwani†  
*Department of Physics, Vanderbilt University, Nashville, Tennessee 37235*

R. L. Robinson and H. J. Kim  
*Oak Ridge National Laboratory, Oak Ridge, Tennessee 37830*  
 (Received 31 July 1978)

The energy levels in  $^{74}\text{Se}$  produced in the  $^{60}\text{Ni}(^{16}\text{O}, 2p)$ ,  $^{64}\text{Ni}(^{12}\text{C}, 2n)$  and  $^{65}\text{Cu}(^{11}\text{B}, 2n)$  reactions were studied. An energy level scheme was deduced from  $\gamma$ - $\gamma$  coincidence measurements. Spin and parity assignments based on angular distribution and directional correlation of oriented nuclei measurements were made for most of the levels. Lifetimes of many of the transitions in  $^{74}\text{Se}$  were deduced from their Doppler broadened lineshapes via the Doppler shift attenuation method. Three "rotational-like" band structures to high spin were observed and their properties investigated. A positive parity,  $\Delta J = 1$ , band to  $(9^+)$  as well as the positive parity,  $\Delta J = 2$ , yrast band to  $(14^+)$  were observed. In addition a negative parity,  $\Delta J = 2$ , band with rotational-like character was seen to  $(13^-)$ .

[ NUCLEAR REACTIONS  $^{60}\text{Ni}(^{16}\text{O}, 2p)$ ,  $E = 45$  MeV;  $^{64}\text{Ni}(^{12}\text{C}, 2n)$ ,  $E = 39$  MeV;  
 $^{65}\text{Cu}(^{11}\text{B}, 2n)$ ,  $E = 29$  MeV,  $^{74}\text{Se}$  levels deduced.  $\gamma(\theta)$ ,  $\gamma$ - $\gamma(\theta)$ ,  $t_{1/2}$  from DSAM.  
 Enriched targets. ]

### I. INTRODUCTION

The ground states of the nuclei in the region between the closed shells at  $Z=N=28$  and  $N=50$  have generally been considered to have near spherical ground states. The level structure has, therefore, been most commonly interpreted in the vibrational picture. However, recent studies of  $^{72,74}\text{Se}$  (Refs. 1-3) by the Vanderbilt ORNL group indicate that the anomalous spacings of the low-lying levels may be understood in terms of the coexistence of the ground-state vibrational band with a  $K=0$  rotational band which is assumed to be built on the low-lying first excited  $0^+$  state. This band is thought to be associated with a second (deformed) minimum in the potential energy surface.

While the low-spin states in  $^{74}\text{Se}$  have been the subject of several investigations,<sup>3-7</sup> information on the high-spin states is needed to further test our understanding of the nuclei in this mass region. The yrast band and  $\Delta J=2$  negative parity band discussed in this paper have been reported in a previous letter.<sup>8</sup> In addition to reporting further details of our investigation of  $^{74}\text{Se}$ , we also report here a  $\Delta J=1$  positive parity band and a band whose spins have not been determined as well as many other levels seen for the first time in beam. Simultaneously the properties of the yrast cascade were studied to high spin by Halbert *et al.*<sup>9</sup> We have observed 60 transitions and es-

tablished 39 excited energy levels from detailed spectroscopy following  $^{60}\text{Ni}(^{16}\text{O}, 2p)$ ,  $^{64}\text{Ni}(^{12}\text{C}, 2n)$ , and  $^{65}\text{Cu}(^{11}\text{B}, 2n)$  reactions. Spins and parities are assigned to many of the levels on the basis of angular distribution and directional correlation of oriented nuclei (DCO) measurements. Lifetimes for ten levels have been deduced from line-shape analyses of transitions depopulating these levels. Bandlike  $\gamma$ -ray cascades are pointed out and their properties discussed. Evidence for rotational character in three of the bands is reported.

### II. EXPERIMENTS

The coincidence data were taken in the  $^{60}\text{Ni}(^{16}\text{O}, 2p)$  reaction studies. The  $^{74}\text{Kr} + 2n$  and  $^{74}\text{Br} + pn$  channels were also seen in this reaction. These latter two residual nuclei  $\beta^+$  decay with half-lives short ( $\sim < 45$  min) compared to our run times and therefore contribute to the  $\gamma$ -ray intensities in  $^{74}\text{Se}$ . Unfortunately, the decay of the  $(4^-)$  isomer in  $^{74}\text{Br}$  modified to an unknown degree the  $\gamma$ -ray anisotropies up through spins 4-6. Thus we instead measured the angular distributions by using the  $^{64}\text{Ni}(^{12}\text{C}, 2n)$  reaction. We attempted to resolve some of the ambiguities in these data with a later experiment in which the  $^{65}\text{Cu}(^{11}\text{B}, 2n)$  reaction was used but found little improvement except in isolated cases.

The heavy ions used in these experiments were produced in the Oak Ridge National Laboratory

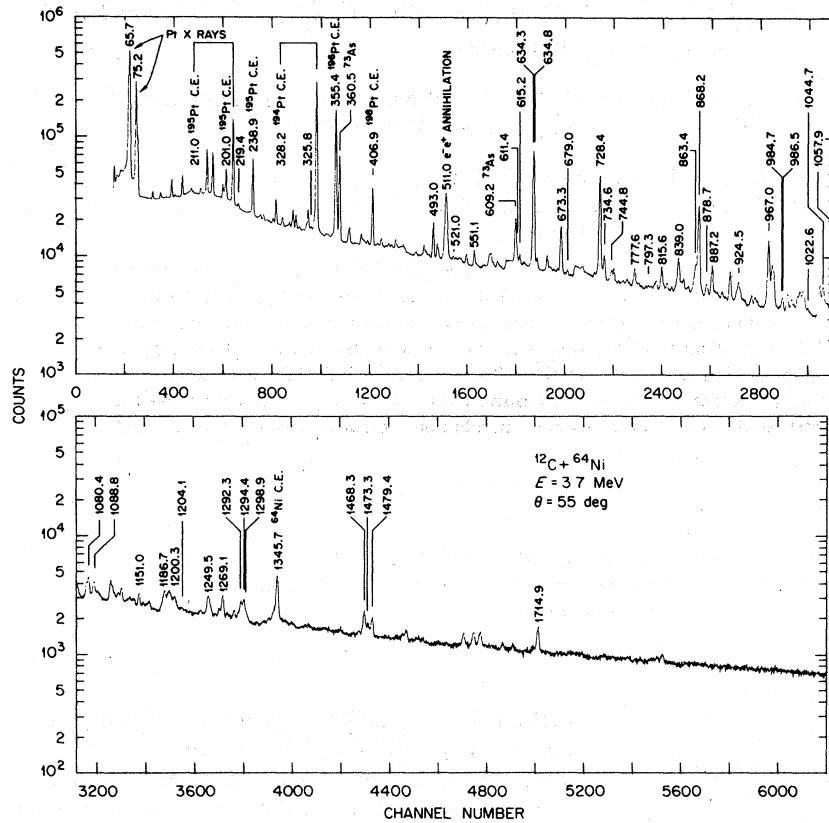


FIG. 1.  $\gamma$ -ray spectrum taken in-beam,  $^{12}\text{C} + ^{64}\text{Ni}$ :  $E = 37$  MeV.

Van de Graaff accelerator. The beam energies for the  $^{16}\text{O}^{(6+)}$ ,  $^{12}\text{C}^{(5+)}$ , and  $^{11}\text{B}^{(4+)}$  were 45, 39, and 29 MeV, respectively. The  $^{60}\text{Ni}$ ,  $^{64}\text{Ni}$ , and  $^{65}\text{Cu}$  targets were enriched to 99.8, 98.0, and 99.7 percent, respectively. In the  $^{60}\text{Ni}(^{16}\text{O}, 2p)$  reaction, singles data were taken at  $0^\circ$ ,  $35^\circ$ ,  $55^\circ$ , and  $90^\circ$ . Coincidence data were taken in the form of selected preset gated spectra with 4096 channels and in a 1024 by 1024 matrix. Singles data only were taken for the  $^{64}\text{Ni}(^{12}\text{C}, 2n)$  and  $^{65}\text{Cu}(^{11}\text{B}, 2n)$  reactions. In these two reactions the data were taken at  $0^\circ$ ,  $55^\circ$ , and  $90^\circ$ , and the reaction was monitored by a second detector at  $270^\circ$  for normalization purposes. Figure 1 shows the  $55^\circ$  singles data taken from the  $^{64}\text{Ni}(^{12}\text{C}, 2n)$  reaction. In all three reactions, Ge(Li) detectors were used. Energy and efficiency calibrations were done with RaE sources.

### III. ANALYSIS AND RESULTS

The results of the  $\gamma$ - $\gamma$  coincidence measurements are summarized in Table I. Many weaker lines which are present in the gates are omitted, and the results of summing gates to improve statistics are also not presented in the table. A hyphen

separating two energies indicate that the  $\gamma$ -ray lines were too close to resolve. Figure 2 shows a sample of the  $\gamma$ - $\gamma$  coincidence data. The spectra have been background subtracted. The decay scheme of  $^{74}\text{Se}$  extracted from these data is shown in Fig. 3. The levels are organized to point out the band structure, and the wider arrows indicate stronger transition intensities. The intensities, given in parentheses, are from the  $^{64}\text{Ni}(^{12}\text{C}, 2n)$  reaction to eliminate  $\beta$  sidefeeding and therefore do not correspond to the intensities in the  $\gamma$ - $\gamma$  coincidence data. The transitions labeled in Fig. 3 with intensities " $< 0.1$ " have significant intensities in the  $^{60}\text{Ni} + ^{16}\text{O}$  reaction from the decay of  $^{74}\text{Br}$ . These transitions also have been seen in previous studies of the low<sup>10</sup> and high<sup>4</sup> spin isomers of established decays of  $^{74}\text{Br}$ .

Angular distribution coefficients were extracted for the stronger lines (which are not complicated by the presence of other nearby lines) by solving the function  $W(\theta) = a_0[1 + Q_2 \alpha_2 A_2 P_2(\theta) + Q_4 \alpha_4 A_4 P_4(\theta)]$ , simultaneously for the three angles, where  $W(\theta)$  is the  $\gamma$ -ray intensity,  $Q_\lambda$ 's are the solid angle corrections,  $\alpha_\lambda$ 's are the alignment parameters as defined in Ref. 11 and  $A_\lambda$ 's are angular distribution coefficients. The initial spins correspond-

TABLE I. Coincidence relations for the  $\gamma$ -ray transitions in  $^{74}\text{Se}$ .

Gate	Lines found in the coincidence spectra
219.4	495?, 634.3-634.8, 651?, 984.7-986.5, 1460.3
325.8	634.3-634.8, 673.3, 728.4, 734.6
493.0	325.8, 634.3-634.8, 673.3, 782.4, 887.2, 984.7-986.5, 1080.4, 1269.1, 1714.9
521.0	634.3-634.9, 728.4, 777.6
551.1	634.3-634.8, 673.3, 728.4, 868.2, 887.2
615.2	634.3-634.8, 679.0, 777.6, 863.4, 924.5, 1269.1, 1366.6
634.3-634.8	219.4, 325.8, 493.0, 551.1, 615.2, 634.3-634.8, 673.3, 728.4, 744.8, 777.6, 815.6, 839.0, 868.2, 878.7, 887.2, 967.0, 984.7-986.5, 1022.6, 1044.7, 1057.9, 1080.4, 1151.0, 1186.7, 1200.3, 1249.5, 1294.4, 1332?, 1366.6, 1455.2, 1460.3, 1468.3, 1473.3, 1649.2, 1679.3, 1714.9, 1842.9, 1890.2, 1928.8, 2283.4, 2310.8, 2333.0, 2387.9
673.3	219.4, 493.0, 611.4, 634.3-634.8, 728.4, 734.6, 868.2, 887.2, 1080.4, 1088.8, 1269.1, 1460.3, 1714.9
679.0	615.2, 634.3-634.8, 728.4, 1249.5
728.4	493.0, 551.1, 634.3-634.8, 673.3, 734.6, 744.8, 815.6, 868.2, 887.2, 924?, 967.0, 984.7-986.5, 1057.9, 1151.0, 1200.3, 1298.9, 1455.2, 1468.3, 1479.4, 1714.9, 1837.1, 1890.2, 2310.8
734.6	634.3-634.8, 673.4, 728.2, 839.0, 887.2, 1269.1, 1473.3
744.8	634.3-634.8, 673.4, 728.4, 734.6, 878.7
777.6	521.0, 615.2, 634.3-634.8, 728.4, 863.4, 1249.5, 1269.1
815.6	551.1, 634.3-634.8, 728.4, 868.2, 1151.0, 1468.3
839.0	634.3-634.8, 673.4, 734.6, 878.7, 887.2, 1269.1, 2333.0, 2387.9
863.4	611.4, 634.3-634.8, 728.4, 924.5, 1249.5, 1298.9
868.2	611.4, 634.3-634.8, 673.4, 728.4, 887.2, 967.0, 1057.9, 1151.0, 1186.7, 1200.3, 1249.5, 1294.4
878.7	634.3-634.8, 728.2, 744.8, 839.4, 1269.1, 1473.3
887.2	493.0, 634.3-634.8, 673.4, 728.4, 734.6, 829.0, 868.2, 1080.4, 1088.8, 1269.1, 1714.9
924.5	615.2, 634.3-634.8, 728.4, 734.6, 777.6, 863.4, 1186.7, 1249.5, 1294.4, 1298.9
967.0	634.3-634.8, 728.4, 868.2, 1057.9, 1186.7
984.7-986.5	219.4, 493.0, 634.3-634.8, 673.4, 728.4, 887.2
1022.6	634.3-634.8
1044.7	634.3-634.8
1057.9	634.3-634.8, 728.4, 868.2, 967.0, 1186.7
1080.4	493.0, 634.3-634.8, 673.4, 1269.1
1088.8	493.0, 634.3-634.8, 673.4, 728.4, 887.2
1151.0	634.3-634.8, 728.4, 815.6, 868.2
1186.7	634.3, 728.4, 868.2, 976.0, 1057.9, 1249.5?, 1292.3
1200.3	634.3-634.8, 728.4
1249.5	634.3-634.8, 679.0, 777.6, 863.4, 1366.0
1292.3-1294.4	634.3-634.8, 728.4, 868.2, 1269.1
1298.9	634.3-634.8, 728.4, 863.4
1366.6	615.2, 634.3-634.8, 1249.5
1455.2	634.3-634.8, 728.4
1468.3	551.1, 634.3-634.8, 728.4, 815.6
1473.3	634.3-634.8
1679.3	634.3-634.8
1714.9	493.0, 634.3-634.8, 673.3, 728.4, 887.2
1837.1	634.3-634.8, 728.4, 984.7-986.5
1842.9	634.3-634.8
1890.2	634.3-634.8, 728.4
2283.4	634.3-634.8
2310.8	634.3-634.8, 728.4
2333.0	734.3-634.8, 829.0, 1473.3
2387.9	634.3-634.8, 728.4, 839.0

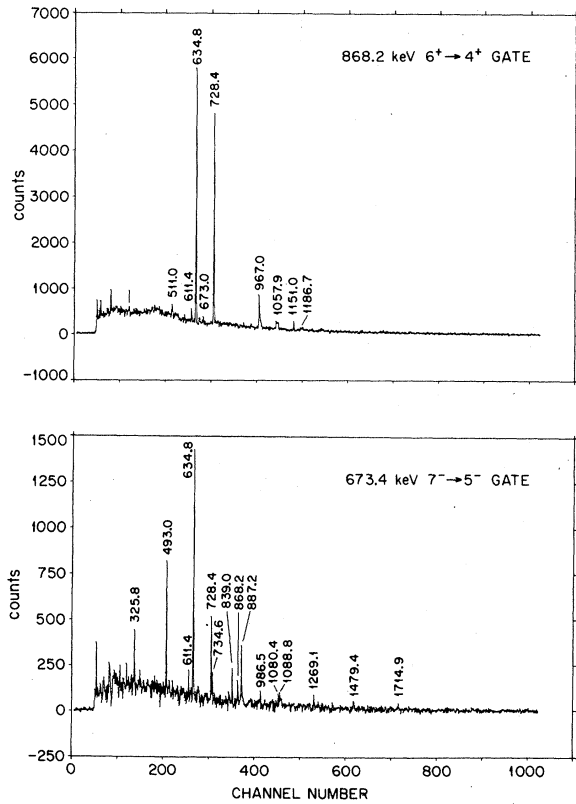


FIG. 2.  $\gamma$ - $\gamma$  coincidence spectra of transitions in  $^{74}\text{Se}$  with a resolving time of  $\approx 30$  nsec.

ing to the best fits of the angular distribution data are given in Table II. Spin assignments were made by fitting the  $A_{\lambda}^{\text{exp}}$ 's to calculated coefficients for different  $\alpha_{\lambda}$ 's and  $\delta$ 's where  $\delta = \langle ||L+1|| \rangle / \langle ||L|| \rangle$  in the phase notation of Biedenharn and Rose,<sup>12</sup> where  $L$  is the lowest possible multipolarity. Such calculations depend on the known final spins.

Table II shows that even when the  $A_2$ 's and  $A_4$ 's are known quite accurately it is often not possible to assign unique initial spins. Additional information may be obtained from the  $\gamma$ - $\gamma$  coincidence data by measuring the ratio of the  $\gamma$ - $\gamma(\Theta)$  correlation in the  $0^\circ$ - $90^\circ$  and  $90^\circ$ - $0^\circ$  geometries, i.e.,

$$R = \frac{W(0^\circ, 90^\circ)}{W(90^\circ, 0^\circ)}.$$

Such a DCO (directional correlation of oriented nuclei) ratio is sensitive in general to both the spin sequence and the  $\delta$ -mixing parameter.<sup>13</sup> Table II also gives the DCO ratio and  $\delta$ -mixing parameter for spin sequences corresponding to the possible initial spins given in Table II. By comparing the calculated and experimental ratios, one can, in some cases, resolve the ambiguities in the spin assignments made from the angular distribution measurements.

Table III summarizes the arguments used to assign spins and parities in  $^{74}\text{Se}$ . The column headed " $\gamma(\Theta), \gamma$ - $\gamma(\Theta)$ " gives the initial spins which are in agreement with the angular distri-

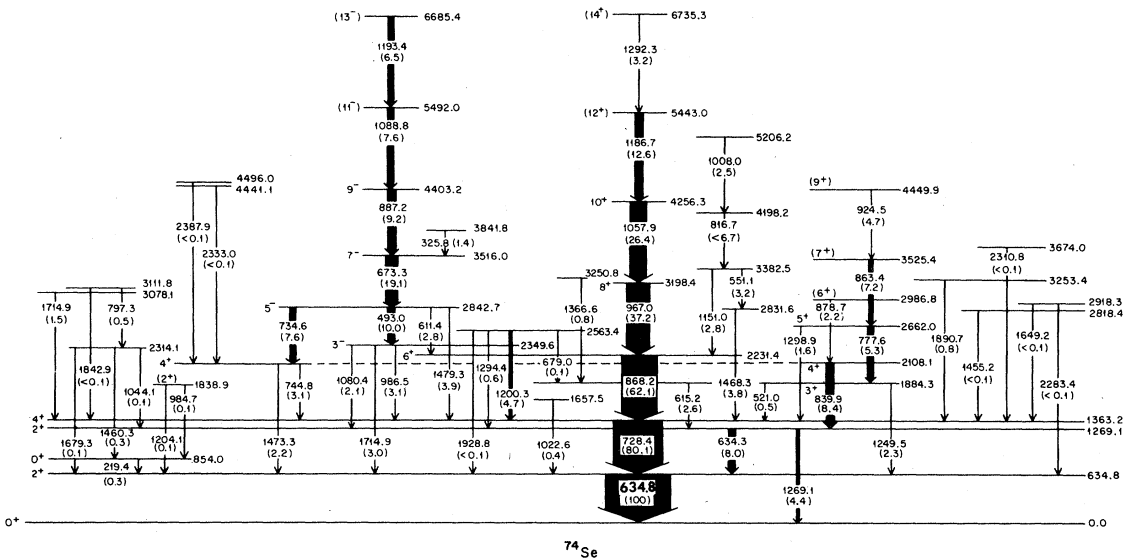


FIG. 3. Levels in  $^{74}\text{Se}$  populated via the  $^{16}\text{O} + ^{60}\text{Ni}$  reactions including in beam and radioactivity levels are shown. The intensities are from the  $^{12}\text{C} + ^{64}\text{Ni}$  reaction and therefore reflect only the in beam,  $^{64}\text{Ni}(^{12}\text{C}, 2n)^{74}\text{Se}$ , population of the levels.

TABLE II. Angular distribution and DCO measurements in  $^{74}\text{Se}$ .

$E_{\text{level}}$	$E_{\gamma}$	$A_2$	$A_4$	$J^{\pi}$ final	Allowed initial	$\delta$	$E_{\gamma_2}$ (gates)	Assumed spin sequence	$R_{\text{exp}}$	$R_{\text{the}}$
1363.2	728.4	0.30(2)	-0.04(2)	2 <sup>+</sup>	2	2.1(2)	634.8	2→2→0	1.05(7)	0.51(2)
					4	0.0		4→2→0		1.00
1884.3	615.2	0.39(10)	-0.03(10)	2 <sup>+</sup>	2	-0.1(1)	1269.1	2→2→0	1.10(15)	1.2(2)
					3	0.3(1)		3→2→0		1.2(3)
					4	0.0		4→2→0		1.00
2108.0	839.0	0.31(3)	-0.06(3)	2 <sup>+</sup>	2	2.2(2)	1269.1	2→2→0	1.08(10)	0.52(2)
					4	0.0		4→2→0		1.00
2231.4	868.2	0.31(2)	-0.09(2)	4 <sup>+</sup>	4		728.9	4→4→2	1.03(6)	0.83(3)
					6			6→4→2		1.00
2349.6	1714.9	-0.30(4)	0.02(4)	2 <sup>+</sup>	1	-0.20(5)				
					3	0.02(5)				
2662.0	777.6	0.25(6)	-0.04(6)	3 <sup>+</sup>	3	1.3(3)				
					5	0.0				
2842.7	493.0	0.32(2)	-0.09(2)	3 <sup>-</sup>	3	0.8(1)				
					5	0.0				
3198.4	967.0	0.43(5)	-0.08(5)	6 <sup>+</sup>	6	0.6(1)	862.2+728.4	6→6→4→2	0.91(8)	0.84(2)
					8	0.0		8→6→4→2		1.00
3516.0	673.3	0.34(2)	-0.07(2)	5 <sup>-</sup>	5	0.78(7)	493.6	5→5→3	1.00(11)	0.84(3)
					7	0.0		7→5→3		1.00
4256.3	1057.9	0.41(4)	-0.08(4)	8 <sup>+</sup>	8	0.5(1)	967.0+868.2	8→8→6→4→2	0.93(7)	0.86(2)
					10	0.0	+728.4	10→8→6→4→2		1.00
4403.2	887.1	0.39(6)	-0.14(6)	7 <sup>-</sup>	7	0.7(1)	673.4+493.0	7→7→5→3	0.91(13)	0.91(7)
					9	0.0		9→7→5→3		1.00
5443.0	1186.9	0.29(8)	-0.11(8)	10 <sup>+</sup>	8	0.0				
					10	0.73				
					12	0.0				
5492.0	1088.8	0.34(14)	-0.21(4)	9 <sup>-</sup>	9	0.8(3)				
					11	0.0				

TABLE III. Spin/parity assignments in  $^{74}\text{Se}$ . References to previous assignments are given in brackets. The previous assignments of the high spin state 10<sup>+</sup>-18<sup>+</sup> in Ref. 9 are based on systematics since their data have the same ambiguity as our data in not excluding a lower spin for  $\delta \sim 0.6$ . We have been more cautious and kept the parentheses at  $I \geq 12^+$ . Parentheses on a decay mode assignment means it is based on the absence of certain transitions which is a weaker argument.

$E_{\text{level}}$	$E_{\gamma}$	$\gamma(\theta)$ DCO	Decay mode	Expected from systematics	Previous assignments	Adopted $J^{\pi}$	$\delta$
	634.8	634.8	1, 2	2 <sup>+</sup>	2 <sup>+</sup> [4]	2 <sup>+</sup>	0
	854.2	219.4	$\leq 4$	0 <sup>+</sup> , 2 <sup>+</sup>	0 <sup>+</sup> [4, 6]	0 <sup>+</sup>	0
	1269.1	634.3	2-4	0, 2, 4	2 <sup>+</sup> [4]	2 <sup>+</sup>	
		1269.1					
	1363.2	728.4	4 <sup>+</sup>	$\leq 4$	4 <sup>+</sup> [4]	4 <sup>+</sup>	0
	1657.5	1022.6		$\leq 4$			
	1838.9	1204.1	1, 2 <sup>+</sup>		2 <sup>+</sup> [4]	(2 <sup>+</sup> )	
		984.7					
	1884.3	5521.0					
		615.2 <sup>a</sup>	2, 3, 4 <sup>+</sup>	2 <sup>+</sup> , 3, 4 <sup>+</sup>	(3, 4)[4] 3 <sup>+</sup> [13]	3 <sup>+</sup>	
		1249.5					
	2108.1	744.8					
		839.0	4 <sup>+</sup>	2, 3, 4 <sup>+</sup>	(3 <sup>+</sup> , 4 <sup>+</sup> )[4]	4 <sup>+</sup>	0
		1473.3					

TABLE III. (Continued).

$E_{\text{level}}$	$E_{\gamma}$	$\gamma(\theta)$ DCO	Decay mode	Expected from systematics	Previous assignments	Adopted $J^{\pi}$	$\delta$
2231.4	868.2	6 <sup>+</sup>		6 <sup>+</sup>	6 <sup>+</sup> [4]	6 <sup>+</sup>	
2314.1	1044.7						
	1460.3		1, 2 <sup>+</sup>		2 <sup>+</sup> [4]	(2 <sup>+</sup> )	
	1679.3						
2349.6	986.5						
	1080.4		2 <sup>+</sup> , 3, 4 <sup>+</sup>		(3 <sup>-</sup> )[7]	3 <sup>-</sup>	
	1714.9	1, 3					-0.08(8)
2563.4	679.0						
	1200.3		2 <sup>+</sup> , 3, 4 <sup>+</sup>				
	1294.4						
	1928.8						
2662.0	777.6	3, 5		5 <sup>+</sup>	5 <sup>+</sup> [13]	5 <sup>+</sup>	
	1298.9						
2818.4	1455.2						
2831.6	1468.3						
2842.7	493.0	3, 5 <sup>-</sup>					
	611.4		5 <sup>-</sup>			5 <sup>-</sup>	
	734.6						
	1479.3						
2918.3	1649.2		2 <sup>+</sup> , 3, 4 <sup>+</sup>				
	2283.4						
2986.8	878.7		(6 <sup>+</sup> )	6 <sup>+</sup>		(6 <sup>+</sup> )	
3078.1	1714.9						
3111.8	797.3		2 <sup>+</sup> , 3, 4 <sup>+</sup>				
	1842.9						
3198.4	967.0	6, 8		8 <sup>+</sup>	8 <sup>+</sup> [9]	8 <sup>+</sup>	
3250.8	1366.6						
3253.4	1890.7						
3382.5	551.1						
	1151.0						
3516.0	673.3	7		7 <sup>-</sup>		7 <sup>-</sup>	
3525.4	863.4		(7 <sup>+</sup> )	7 <sup>+</sup>		(7 <sup>+</sup> )	
3674.0	2310.8						
3841.8	325.8		5-9				
4198.0	815.6						
4256.3	1057.9	8, 10		10 <sup>+</sup>	10 <sup>+</sup> [9]	10 <sup>+</sup>	0
4403.2	887.2	7, 9		9 <sup>-</sup>		9 <sup>-</sup>	0
4441.1	2333.0				(4 <sup>-</sup> , 3 <sup>-</sup> )[4]		
4449.9	924.5		(9 <sup>+</sup> )	9 <sup>+</sup>		(9 <sup>+</sup> )	
4496.0	2387.9				(4 <sup>-</sup> , 3)[4]		
5443.0	1186.7	8, 10, 12		12 <sup>+</sup>	12 <sup>+</sup> [9]	(12 <sup>+</sup> )	(0)
5492.0	1088.8	9, 11		11 <sup>-</sup>		11 <sup>-</sup>	0
6685.4	1193.4		(13)	13 <sup>-</sup>		(13 <sup>-</sup> )	
6735.3	1292.3				14 <sup>+</sup> [9]	(14 <sup>+</sup> )	

bution and DCO measurements. The "decay mode" column gives those spins which are possible with the assumption that the  $\gamma$  rays observed correspond to  $\Delta J \leq 2$ . Most spin assignments are unique on the basis of these two columns. Parity assignment are made assuming that multipoles no higher than  $E2$  will be present in the coincidence data and that no large  $M2$  strengths will be present. For the high-spin states of the prominent cascades, argu-

ments are based on the systematics of the cascades and similar cascades in other nuclei. In the case of the levels at 1884.3 and 2349.6 keV, we draw from previous works as referenced in the "previous assignments" columns. All the levels and transition energies are given in the table for convenience, although little is known about the spins in many cases.

Ten of the  $\gamma$  rays which we have placed in  $^{74}\text{Se}$

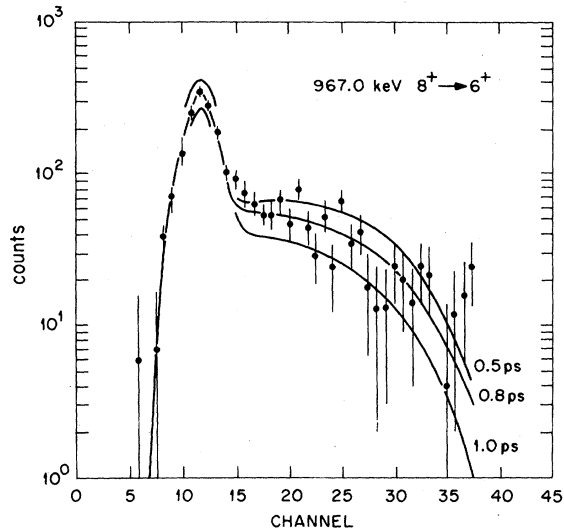


FIG. 4. Fits to the Doppler broadened lineshape of the 967.0 keV transition in  $^{74}\text{Se}$ . The lineshape was taken from the coincidence spectra to eliminate side feeding and possible contaminants.

exhibit sufficient Doppler shifting in the forward angles to allow lifetimes to be extracted via the DSAM method. The Doppler shifts have been identified by examining the angular dependence of the line shapes in the singles data; however, the fits must be done in the coincidence data to isolate and properly compensate for side feeding. (Any lifetimes associated with any side feeders were not considered in Ref. 9.) Figure 4 shows an example of a computer fit and illustrates the sensitivity of the line shape to the lifetime of the depopulated level. Table IV summarizes our result for the lifetimes of the levels in  $^{74}\text{Se}$  and compares them to other measurements.

#### IV. DISCUSSION

In the decay scheme (Fig. 3), three well-defined bands are seen to high energy with definite or tentative spins and parities and with no crossing transitions between the higher spin members (note the tentative assignments are strongly favored by the data). A fourth band is also seen emerging at the 2831.6 or 3382.5 keV levels but unfortunately

TABLE IV. Mean lives of levels in  $^{74}\text{Se}$ . The present results were also reported in Ref. 8.

Transition energy (keV)	Level	$J_i^\pi \rightarrow J_f^\pi$	Present studies $\tau_m(\text{ps})$	Previous studies $\tau_m(\text{ps})$	$\frac{B(E2)}{B(E2)_{\text{sp.,w}}}$	$ \beta $
634.8	634.8	$2^+ \rightarrow 0^+$		10.7(4) <sup>b</sup>	$40(\pm 2)$	0.30(1)
728.4	1363.2	$4^+ \rightarrow 2^+$		2.7(1) <sup>b</sup>	81(3)	0.35(1)
868.2	2231.4	$6^+ \rightarrow 4^+$	2.40(30)		$38(\pm 6)$	0.23(1)
967.0	3198.4	$8^+ \rightarrow 6^+$	0.80(10)	0.96(10) <sup>c</sup>	$66(\pm 3)$	0.30(2)
1057.9	4256.3	$10^+ \rightarrow 8^+$	0.53(10)	0.70(10) <sup>c</sup>	$75(\pm 15)$	$0.27(\pm 3)$
1186.7	5443.0	$(12^+) \rightarrow 10^+$	0.30(15)	0.41(5) <sup>c</sup>	$63(\pm 6)$	$0.28(\pm 12)$
1292.3	6735.3	$(14^+) \rightarrow (12^+)$	0.35(15)	0.31(5) <sup>c</sup>	$36(\pm 26)$	$0.21(\pm 7)$
673.3	3516.0	$7^- \rightarrow 5^-$	5.0(20)		$64(\pm 43)$	$0.30(\pm 3)$
887.2	4403.2	$9^- \rightarrow 7^-$	0.70(20)		$116(\pm 46)$	$0.38(\pm 7)$
1088.8	5492.0	$(11^-) \rightarrow 9^-$	0.40(5)		$78(\pm 14)$	$0.30(\pm 3)$
863.4	3525.4	$(7^+) \rightarrow 5^+$	0.70(30)		$133(\pm 35)$	$0.42(\pm 5)$
924.5	4449.9	$(9^+) \rightarrow (7^+)$	0.60(20)		$111(\pm 35)$	$0.38(\pm 7)$
219.4	854.2	$0^{+'} \rightarrow 2^+$	1200(200) <sup>a</sup>	1019(68) <sup>b</sup>	$83(\pm 6)$ <sup>d</sup>	0.19(1)
1269.1	1269.1	$2^{+'} \rightarrow 0^+$		$5.6(\pm 2.7)$ <sup>b</sup>	2(1)	0.07(1)

<sup>a</sup> Ronningen *et al.*, Ref. 3.

<sup>b</sup> Barrette *et al.*, Ref. 7.

<sup>c</sup> Halbert *et al.*, Ref. 9 [excludes any lifetimes associated with any side feeders. Thus these data were not included in calculating  $B(E2)$  values].

<sup>d</sup> Calculated from a weighted average (=1065 ps).

the spins and parities are not established. The positive parity yrast band, yb, is shown to  $(14^+)$  and a negative parity band, npb, that starts at the  $3^-$  octupole state<sup>5</sup> is shown to  $(13^-)$ .

The third strong band clearly emerges above the  $3^+$ , 1884.3 keV state. Except for the  $3^+$  assignment of the 1884.3 keV state, the spin/parities in Fig. 3 are from our studies, with the understanding that the  $5^+$ ,  $(7^+)$  and  $(9^+)$  assignments are based on the  $3^+$  assignment from Ref. 14. The  $3^+$  and  $4^+$  members of this band and the 1269.1 keV  $2^+$  level have been interpreted as members of a quasi- $\gamma$  band<sup>14</sup> (qgb). However, there are other candidates for the  $2^+$  member of this band, for example the 1657.5 keV level. As seen in Fig. 5 where the energies of this band are plotted vs  $J(J+1)$ , an energy of 1400–1500 keV for the  $2^+$  member looks more reasonable. There could be mixing of this band's  $2^+$  member with other  $2^+$  states that could shift the energies up or down. This is the first time that a band with the characteristics (see Figs. 3, 5) or a  $\gamma$ -type vibration in a well-deformed nucleus has been suggested to so high a spin in this mass region. In the quasi- $\gamma$  band picture of Sakai,<sup>15</sup> the states earlier reported<sup>14</sup> up through spins 5 or 6 are interpreted as selected members of the two-, three-, and four-phonon states. The extension of this band to spins of  $(9^+)$  would then come out of the five- and six-phonon states. The extension of this quasi- $\gamma$  picture to such high phonon states when even well-behaved two-phonon triplets are hard to find would seem questionable. Also if these are selected members of successively higher phonon states, there is the question of why one does not see branching from states in this band to other members of the next lower phonon multiplet which are located in this third band and in the yrast band in the quasiband picture.<sup>15</sup> In Figs. 3 and 5 one notes that in fact this band breaks up into two bands,  $(9^+) \rightarrow (7^+) \rightarrow 5^+ \rightarrow 3^+$  and  $(6^+) \rightarrow 4^+$ . The staggering, however, is smaller than expected in the quasi- $\gamma$  band where the  $3^+$  and  $4^+$  members,  $5^+$  and  $6^+$  members and so on are from the same phonon multiplet and is more in line with the odd-even staggering observed in  $\gamma$  bands in well-deformed nuclei. Of course, Sakai's<sup>15</sup> quasi- $\gamma$  band picture is not a pure phonon model but has large anharmonicities so one can adjust the splittings.

Only  $\Delta J = 2$  transitions are observed in this third band, and where the mean lives are measured they are highly collective (see Table IV). If equal  $B(E2)$  values are assumed, transitions such as the  $(7^+) \rightarrow (6^+)$ ,  $(6^+) \rightarrow 6^+$ ,  $5^+ \rightarrow 6^+$ ,  $5^+ \rightarrow 4^+$ , which are allowed by phonon selection rules in that picture,<sup>15</sup> should be but are not observed. The upper limits for their intensities are much smaller than the values predicted on the basis of equal

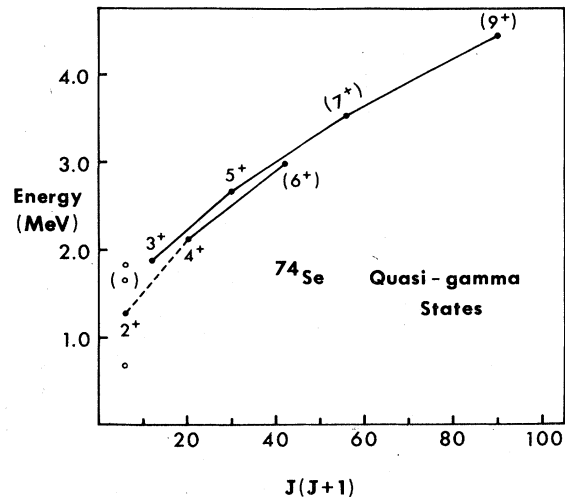


FIG. 5. The level energies vs  $J(J+1)$  are plotted for the  $\Delta J = 1$  positive parity band. Several candidates are shown for the  $2^+$  member of this band.

$B(E2)$  values without even considering that  $\Delta J = 0, 1$  transitions between phonon states typically have up to equal amounts of  $M1$  radiation. Such low intensities for all these  $\Delta J = 0, 1$  transitions and for  $\Delta J = 2$  band crossing ones compared to the very collective  $\Delta J = 2$  ones within the band along with the observance of this band to the  $(9^+)$  member underscores that this is a particularly stable, very collective mode. Thus in terms of the energy spacing and branching ratios this band looks more like a true  $\gamma$  vibrational band in a well-deformed nucleus than a quasi- $\gamma$ , whose levels are members of phonon multiplets. In contrast to the skepticism given Sakai's<sup>15</sup> proposal of quasi- $\gamma$  bands in 1967, this band is now so well established as an important independent collective mode in this region that the word "quasi" may not be the best word to describe these bands.

In Fig. 6 we plot the excitation energies of the yb and the npb as functions of  $J(J+1)$ . In addition the energies of the npb have been fitted to  $E = E_0 + AJ(J+1) + B[J(J+1)]^2$ . Both the plot and the fit as shown in Fig. 6 indicate strong rotational behavior for the npb with very little stretching (i.e.,  $B/A = -1.5 \times 10^{-4}$ ). The large enhancements, 60–116, compared to single particle estimates for the  $E2$  transitions in this band indicate that the levels are highly collective. Rotational structure for the npb band is further indicated in Fig. 7 where the moment of inertia vs  $(\hbar\omega)^2$  is plotted in the standard manner.<sup>16</sup> The near constancy of the moment of inertia for the npb beginning at a known  $3^-$  octupole state along with the highly collective nature of the levels led us earlier to suggest<sup>8</sup> that this was an octupole band. While



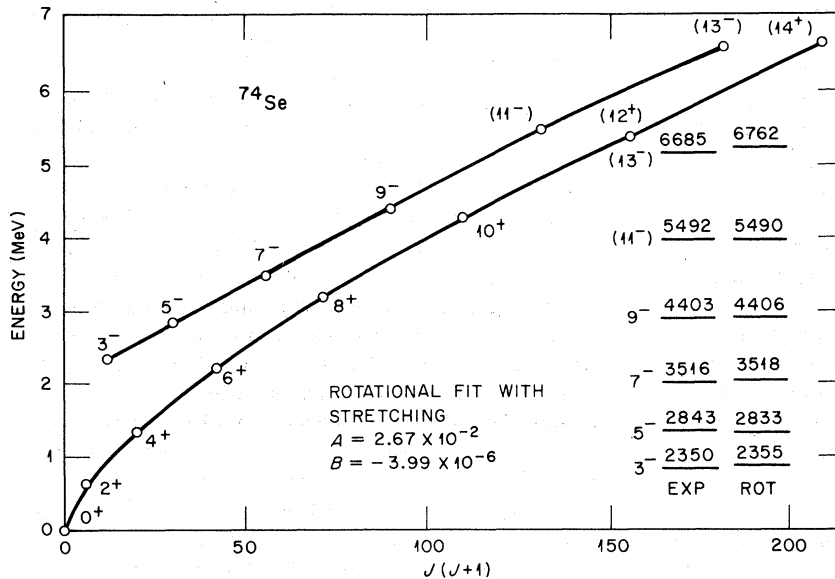


FIG. 6. The level energies vs  $J(J+1)$  are plotted for the yrast and the negative parity bands. The negative parity band is fitted to  $E = E_0 + AJ(J+1) + BJ^2(J+1)^2$  and the values of  $A$  and  $B$  are shown.

this may still be the case, another interpretation has emerged,<sup>17</sup> and it is clearly supported by the npb observed<sup>18</sup> in nearby <sup>78</sup>Kr. Peker and Hamilton<sup>19</sup> have suggested that a more fruitful way to extract information from a band is to plot the second differential function,  $\Delta^2 E = E_{\nu_2} - E_{\nu_1}$ , as a function of the minimum spin in the three states involved. Based on the rotational energy formula derived for deformed nuclei, this function should smoothly decrease with increasing spin.<sup>19</sup> Upward jumps in  $\Delta^2 E$  indicate something has interrupted the normal sequence. For example in rare-earth nuclei, when backbending of the moment of inertia occurs from the crossing of two bands, there is a sudden jump in  $\Delta^2 E$  similar to those seen in Fig. 8. There is a sharp upward rise in  $\Delta^2 E$  for the npb in <sup>74</sup>Se that reflects the small break between 3<sup>-</sup> and 5<sup>-</sup> as seen in Fig. 7. This break has led Peker *et al.*<sup>17</sup> to suggest that the earlier assignment<sup>8</sup> of the npb as a pure octupole band may be too simple and that the npb is complex with a band built on the 3<sup>-</sup> octupole state crossed at the 5<sup>-</sup> level by another band. This second npb, which crosses at 5<sup>-</sup>, they suggest is built on a rotation-aligned, two-particle 5<sup>-</sup> level with configuration  $(g_{9/2}, f_{5/2})$ ,  $(g_{9/2}, p_{3/2})$ , or  $(g_{9/2}, p_{1/2})$ . If this is correct, then the constancy of  $\mathcal{I}$  in Fig. 7 for the npb is an artifact of the crossing. In this picture the 5<sup>-</sup> spin of the band head is then rotational-aligned to rotational states with  $J=0, 2, 4, \dots$  (with energy spacing which track the ground rotational band levels with these spins) to generate the band. In support of this picture, a very similar negative-parity band is seen<sup>18</sup> in <sup>78</sup>Kr, but there the band head is clearly 5<sup>-</sup> with a large energy gap to the

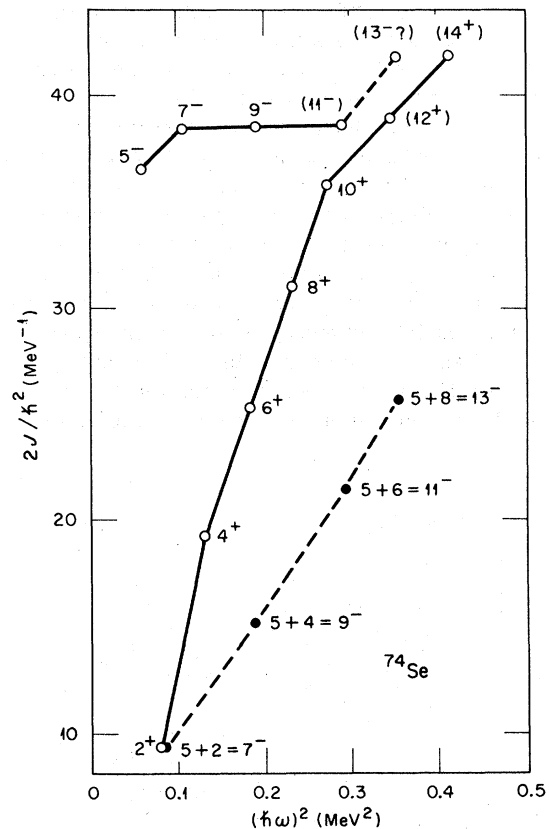


FIG. 7. Moment of inertia plots for the yrast and negative parity bands in <sup>74</sup>Se. The lower dashed line is produced by subtracting 2 units of angular momentum from the total angular momentum for the negative parity band.

$3^-$  state. Further support for the rotational-aligned model is found in the yb in neighboring nuclei in this region as discussed below. Furthermore, if the moment of inertia plot is revised to account for the rotation-alignment nature of this band as indicated in Fig. 7 where spins of 0, 2, 4, ... are used in the rotational energy formula, the moment of inertia of the npb behaves much like the upper part of the yb. Note also that the break seen in Fig. 7 between the  $(11^-)$  and  $(13^-)$  states disappears in the rotation-alignment picture.

Now let us look at the even-parity yb. The curves in Figs. 6 and 7 for the yb are typical of many yrast bands in this mass region. In Fig. 7, the moment of inertia does not show the sharp forward bend at low spin seen<sup>1</sup> in  $^{72}\text{Se}$ , although there is a smaller forward bend at the  $10^+$  state. If one looks at  $\Delta^2 E$  (Fig. 8) for the yb, however, two jumps are observed; one around spin 2-4 and one around spin 8-10. This figure suggests that two band crossings have occurred, although only one is indicated in the moment of inertia plot. The low-lying  $0^+$  and  $6^+$ ,  $8^+$ ,  $10^+$ , and  $12^+$  members of the yb in  $^{72}\text{Se}$  (Ref. 1, 2) have been interpreted in terms of the coexistence of a near-spherical ground band with a  $K=0$  rotational band built on a secondary minimum at larger deformation in the potential energy surface. Because of the similar low energy and enhanced decay of the  $0^+$  excited state, coexistence also has been suggested<sup>3</sup> in  $^{74}\text{Se}$ . The break at low spin in Fig. 8 gives added support to the interpretation<sup>3</sup> that two bands have crossed at low spin in  $^{74}\text{Se}$ , as in  $^{72}\text{Se}$ . Figure 9 shows how one could construct a coexistence model with the  $0^+$ ,  $8^+$ , and  $10^+$  and energies to find the energies of the  $2^+$  and  $4^+$  members of the deformed band. Here the  $2^+$  rotational and  $2^+$  vibrational states could be mixed and one pushed up to 1269.1 keV

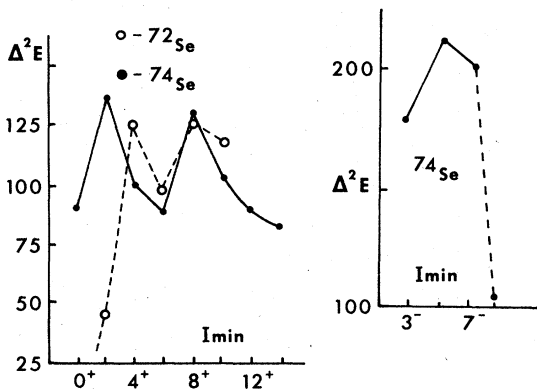


FIG. 8.  $\Delta^2 E$  vs  $J_{\min}$  plots for the yrast bands in  $^{72,74}\text{Se}$  and the negative parity band in  $^{74}\text{Se}$ .

and the other down to 634.8 keV as found experimentally. The  $4^+$  rotational energy is also near the  $4^+$  two-phonon energy predicted from an unperturbed one-phonon energy of 837 keV. If the 1363.2 keV  $4^+$  level is the  $4^+$  deformed state shifted down, then without introducing any anharmonicity which also could shift the vibrational  $4^+$  level, the  $4^+$  vibrational level should be shifted up if equal mixing is assumed to about 1860 keV. The two known nearby states at 1838.9 and 1884.3 have spins of  $(2^+)$  and  $3^+$ , however, and the 1657.5 keV level which could be  $4^+$  seems too low. The only other state definitely assigned as  $4^+$  in this region is at 2108.1 keV, and it appears to be more associated with the more  $\gamma$ -type vibrational band discussed above. If this  $4^+$  state is considered as the  $4^+$  vibrational state which has mixed with the  $4^+$  rotational one, then a large but not unreasonable anharmonicity also has to be introduced. On the other hand, it is possible that the  $4^+$  vibrational state now mixed and shifted simply has not been seen. The absence of some definite conclusion

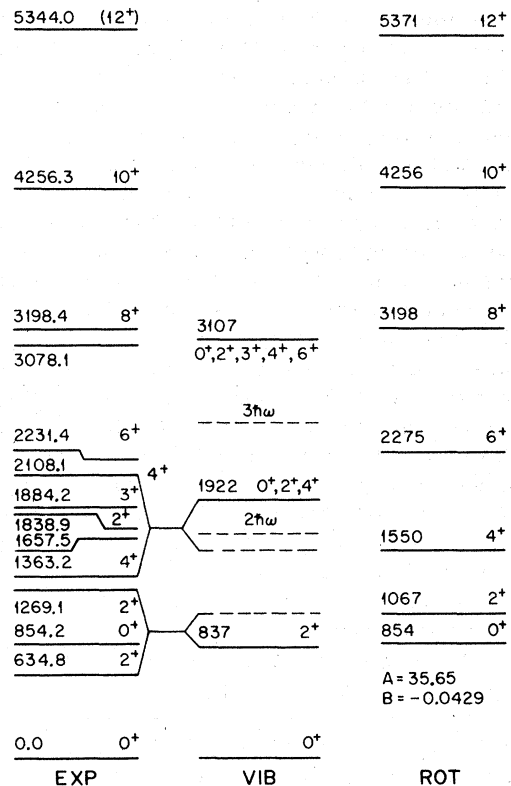


FIG. 9. The figure shows how vibrational and rotational levels can be extracted from the experimental levels of  $^{74}\text{Se}$  by assuming coexistence of spherical and deformed states. The  $0^+$ ,  $8^+$ , and  $10^+$  levels were used to extract the  $A$  and  $B$  and therefore determine the position of the unperturbed  $2^+$  and  $4^+$  rotational states.

about the energy of the second mixed vibrational-rotational  $4^+$  state makes it difficult to proceed further and apply the Gneuss-Greiner<sup>20</sup> approach where one varies the potential energy surface through many different variations to see which reproduces the experimental data the best. If one assumes that the 2108.1 keV,  $4^+$  level is the second member of a mixed  $4^+$  doublet, then the potential energy surface is as shown in Fig. 10. The spectrum is shown in Fig. 11 where only the  $2^+$ ,  $0^+$ ,  $2_2^+$ ,  $4^+$ ,  $4_2^+$ , and  $6^+$  experimental energies and the  $B(E2)$  values were used in the fit. This potential, Fig. 10, is soft to  $\gamma$  deformation and has only a somewhat weak second minimum along the oblate axis at higher deformation. Unfortunately, the energy of the second  $4^+$  level is important in determining which potential energy surface fits the data. If this  $4^+$  energy was about 250 keV lower as in  $^{72}\text{Se}$ , and even deeper minimum at large deformation should be seen. This only serves to underscore that in a given nucleus you can be misled in the Gneuss-Greiner approach by the wrong choice of energy levels. Unless definite assignments are available on a given nucleus, one should be more concerned with the broad trends predicted by the energy surfaces. Despite the ambiguity in obtaining a potential surface for  $^{74}\text{Se}$ , Fig. 8 indicates that the yb in  $^{72}\text{Se}$  and  $^{74}\text{Se}$  are similar with band crossings occurring at the  $2^+$ - $4^+$  levels.

Finally, it is entirely possible, and indeed the second break seen in Fig. 8 supports, that the yb is crossed a second time around spins  $8^+$  to  $10^+$  by still another band. In  $^{68}\text{Ge}$  we have presented strong evidence that the ground-state band is broken off at  $8^+$  by two separate bands.<sup>21</sup> In the rotation-aligned model, one is based on a neutron

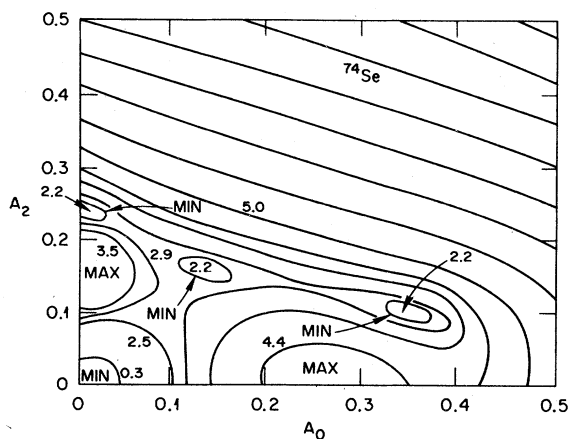


FIG. 10. The potential energy surface (PES) for  $^{74}\text{Se}$  showing spherical and triaxial minima.

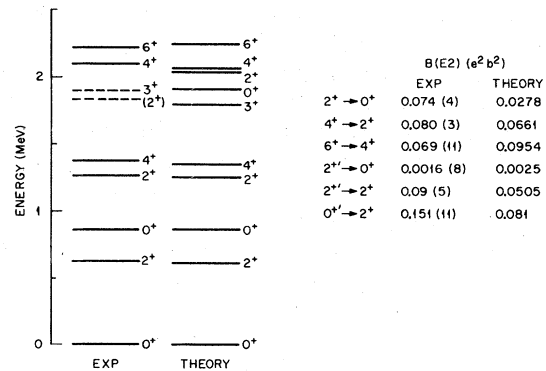


FIG. 11. The energy level fit produced from the PES in Fig. 10. The levels used in the fit are discussed in the text.

( $g_{9/2}$ )<sup>2</sup> and one on a proton ( $g_{9/2}$ )<sup>2</sup> configuration. Such rotation-aligned bands are well established in heavier nuclei such as Pd, Ba and the deformed rare earths.<sup>22,23</sup> If this has occurred in  $^{74}\text{Se}$  also, as indicated by the second jump in Fig. 8, then depending on whether the  $8^+$  ( $g_{9/2}$ )<sup>2</sup> state is above or below the  $8^+$  member of the band it is crossing, the  $8^+$  or  $10^+$  and higher states, are members of a rotational-aligned band. In this case one has essentially no possibility to quantitatively apply the coexistence model since one does not have sufficient levels to obtain the coefficients in the energy expansions to obtain the unperturbed  $2^+$  and  $4^+$  rotational energies as done above. It would also be probable that above  $10^+$  these two bands would have similar energy for equal spin states and could mix at several spins. Finally, we also want to point out that the anomalously low energy of the first excited  $0^+$  state may be related to pairing effects at the  $N=40$  subshell closure as suggested by Haderman and Rester<sup>24</sup> and not to being the band head of a more well-deformed band.

In summary, from Fig. 8 it appears likely that indeed there may be at least two crossing points in the yb that would involve three different bands, the lowest of which is built on a nearly spherical ground state, the highest of which is most probably a rotation-aligned band, and the middle one is more speculative but it may be one built on a more strongly deformed shape from a second minimum in the potential energy surface. It is clear that each of these bands in the yrast line is highly collective based on the large enhancements of the  $E2$  transitions out of these levels as shown in Table IV. The possibility of mixing at many different spins of these multiple bands could explain the differences in the moment of inertia plots of  $^{74}\text{Se}$  and  $^{72}\text{Se}$ . We plan to carry out calculations in the rotation-aligned model<sup>23</sup> to see where one

could expect these bands to be in  $^{72,74}\text{Se}$ . It would also be of interest to use the dynamic deformation model of Kumar *et al.*<sup>25</sup> which has now been applied with good success to the excited  $0^+$  states in  $^{70-74}\text{Ge}$  Ref. 26. In  $^{72}\text{Se}$  it seems that greater clarity of the band structures may be occurred because of better separation of the energies of like spin states except at the  $2^+$  level. Clearly there is a wealth of collective behavior going on, perhaps related to a multitude of nuclear personalities, to

challenge more microscopic calculations in this region.

The research performed at Vanderbilt University was supported in part by grants from the National Science Foundation and the U. S. Department of Energy. The research performed at Oak Ridge National Laboratory was supported in part by the U. S. Department of Energy under contract with Union Carbide Corporation.

\*Present address, Michigan State University, East Lansing, Michigan.

†Present address, Institut für Theoretische Physik der Justus-Liebig-Universität Giessen.

<sup>1</sup>J. H. Hamilton, A. V. Ramayya, W. T. Pinkston, R. M. Ronningen, G. Garcia-Bermudez, R. L. Robinson, H. J. Kim, R. O. Sayer, and H. K. Carter, *Phys. Rev. Lett.* **32**, 239 (1974).

<sup>2</sup>J. H. Hamilton, H. L. Crowell, R. L. Robinson, A. V. Ramayya, W. E. Collins, H. J. Kim, R. O. Sayer, T. Magee, and L. C. Whitlock, *Phys. Rev. Lett.* **36**, 340 (1976).

<sup>3</sup>R. M. Ronningen, A. V. Ramayya, J. H. Hamilton, W. Lourens, J. Lange, H. K. Carter, and R. O. Sayer, *Nucl. Phys.* **A261**, 439 (1976).

<sup>4</sup>A. Coban, J. C. Lisle, G. Murray, and J. C. Willmott, *Part. Nucl.* **4**, 108 (1972).

<sup>5</sup>H. Schmeing, R. L. Graham, J. C. Hardie, and J. S. Geiger, *Nucl. Phys.* **A233**, 63 (1974).

<sup>6</sup>S. Göring and M. V. Hartrott, *Nucl. Phys.* **A152**, 241 (1970).

<sup>7</sup>J. Barrett, M. Barrette, G. Lamoureux, and S. Monaro, *Nucl. Phys.* **A235**, 154 (1974).

<sup>8</sup>R. B. Piercey, A. V. Ramayya, R. M. Ronningen, J. H. Hamilton, R. L. Robinson, and H. J. Kim, *Phys. Rev. Lett.* **37**, 496 (1976).

<sup>9</sup>M. Halbert, P. O. Tjøm, I. Espe, G. B. Hagemann, B. B. Herskind, M. Neiman, and H. Oeschler, *Nucl. Phys.* **A259**, 496 (1976).

<sup>10</sup>A. Coban, *J. Phys. A: Math., Nucl. Gen.*, **7**, 1705 (1974).

<sup>11</sup>T. Yamazaki, *Nucl. Data* **A3**, 1 (1967).

<sup>12</sup>L. C. Biedenharn and M. E. Rose, *Rev. Mod. Phys.* **25**, 729 (1953).

<sup>13</sup>K. S. Krane, R. M. Steffen, and R. M. Wheeler, *Nucl. Data Tables*, **11**, 351 (1973).

<sup>14</sup>N. Yoshikawa, D. Hashimoto, Y. Shida, and M. Sakai, *Proceedings of the International Conference on Selected Topics in Nuclear Structure*, Dubna, USSR, June 1976 (unpublished), p. 77.

<sup>15</sup>M. Sakai, *Nucl. Data Tables* **15**, 513 (1975); and *Proc. Colloque Franco-Japanais de Spectroscopie Nucléaire et Reaction Nucléaire* (Institute for Nuclear Study, Tokyo, 1976), p. 3; *Nucl. Phys.* **A104**, 301 (1976).

<sup>16</sup>R. A. Sorensen, *Rev. Mod. Phys.* **45**, 353 (1973).

<sup>17</sup>L. K. Peker, J. H. Hamilton, A. V. Ramayya, R. B. Piercey, and R. L. Robinson, *Proceedings of the International Conference on Nuclear Structure, Tokyo, 1977*, edited by T. Marumori (Physical Society of Japan, Tokyo, 1978), p. 289.

<sup>18</sup>R. L. Robinson, H. J. Kim, R. O. Sayer, R. B. Piercey, A. V. Ramayya, J. H. Hamilton, and J. C. Wells, *Bull. Am. Phys. Soc.* **22**, 1027 (1977).

<sup>19</sup>L. K. Peker and J. H. Hamilton, *Proceedings of the International Conference on Nuclear Structure* (unpublished), p. 110.

<sup>20</sup>G. Gneuss and W. Greiner, *Nucl. Phys.* **A171**, 449 (1979).

<sup>21</sup>A. de Lima, J. H. Hamilton, A. V. Ramayya, B. van Nooijen, R. M. Ronningen, H. Kawakami, R. B. Piercey, E. de Lima, R. L. Robinson, H. J. Kim, W. K. Tuttle, L. K. Peker, F. A. Rickey and R. Popli, *Phys. Lett.* (to be published).

<sup>22</sup>C. Flaum and D. Cline, *Phys. Rev. C* **14**, 1224 (1976).

<sup>23</sup>C. Flaum and D. Cline, *Nucl. Phys.* **A264**, 291 (1976).

<sup>24</sup>J. Haderman and A. C. Rester, *Nucl. Phys.* **A231**, 120 (1974).

<sup>25</sup>K. Kumar, R. Remand, P. Agner, J. S. Vaager, A. C. Rester, R. Foucher, and J. H. Hamilton, *Phys. Rev. C* **16** (1977).

<sup>26</sup>K. Kumar report (unpublished).